

Plug-in Strategy for Market Introduction of Fresnel-Collectors

Gabriel Morin ^a, Hansjörg Lerchenmüller ^a, Max Mertins ^a,
Dr. Markus Ewert ^b, Mathias Fruth ^c, Dr. Stefan Bockamp ^c, Thomas Griestop ^c
Dr. Andreas Häberle ^d

^a Fraunhofer Institute for Solar Energy Systems, Heidenhofstr. 2, 79110 Freiburg, Germany
e-mail: hansjoerg.lerchenmueller@ise.fraunhofer.de

^b E.ON Energie AG, Brienner Str. 40, 80333 Munich, Germany
e-mail: markus.ewert@eon-energie.com

^c E.ON Engineering GmbH, Bergmannsglückstr. 41-43, 45896 Gelsenkirchen, Germany
e-mail: mathias.fruth@eon-engineering.com

^d PSE GmbH, Solar Info Center, 79072 Freiburg, Germany
e-mail: haeberle@pse.de

Abstract – The market introduction of solar thermal power technologies has two central barriers. On the one hand, the total investments compared to other renewable technologies are very high since solar thermal power stations can only be installed from a size of several 10 MW. On the other hand, solar thermal power projects have a relatively high risk due to limited experience. This applies especially for the Fresnel collector, since this new technology has not yet been proven in full scale size. A plug-in of a solar field in an existing power plant could help by lowering the investment significantly and, at the same time, lowering the risk by using the solar field heat in a first step just for pre heating the feed water.

The paper presents simulation results of Fresnel solar collectors integrated into a fossil fired power plant. The technical solutions will be discussed and a risk assessment will be carried out. Last but not least, the paper shows economic calculations on electricity costs with different assumptions for CO₂-allowances. The results show that the integration of high temperature solar collectors into a conventional large-scale power plant is a very cost efficient way for market introduction of Fresnel collectors. However the solar shares of the investigated variants are low. Therefore the long term strategy must aim at producing live steam parameters in order to generate a significant amount of solar electricity.

1. Introduction

Starting from an existing natural gas fired 630 MW_{el} steam plant in Egypt, different concepts for integrating a Fresnel Collector into the water-steam-cycle of the plant were developed. In all concepts, the solar field is used for feed-water preheating, substituting conventional extraction steam which can remain in the turbine to generate additional electricity.

On the basis of thermodynamic plant data, weather data, and a thermodynamic collector model, the annual solar yield is determined. Besides technical aspects and risks, an important evaluation criterion are the levelized electricity costs (LEC). Therefore plant designs are optimized with regard to this criterion. The Fresnel collector simulated in this paper is a cost-optimized variant of the Solarmundo collector, using one single absorber tube and a secondary mirror system (see Figure 1).

Previous examinations [1] have shown that it is technically and economically more advantageous to integrate a solar field into a conventional steam power plant than into a combined cycle (ISCC – integrated solar combined cycle). The gas fired reference plant used in this case and the integration concepts are exemplary and can also be translated to other large scale conventional steam power plants, like e.g. coal fired power plants. Beyond that, many of the results can also be applied for other solar thermal power technologies, such as parabolic trough plants.



Figure 1: Prototype of the Fresnel collector (2,500 m²) erected by the company Solarmundo, Belgium. On the bottom of the image: the Fresnel mirrors, on top: the collector tube covered by a thermally insulated secondary mirror (source: Solarmundo).

2. Reference Plant and Solar Field Integration Concepts

Starting point for the water-steam-cycle-simulations was the plant data of the 630 MW_{el} plant with an efficiency (fuel to net electricity at full load) of 42.0%.

Based on the heat balance data, different integration concepts with a solar heat input of up to 30 MW_{th} were developed. Design criteria for the variants presented below were:

- efficiency (DNI¹ to electricity),
- pressure losses in the solar field,
- water velocity versus tube length (parallel tubes),
- control aspects,
- and, for the pure water heating variants, security reserve for pressure-dependent boiling conditions.

The water-steam-cycle and the integration variants were modeled with the commercial process simulation program Epsilon [2]. In this paper the following five solar field integration concepts are investigated:

- heating medium pressurized water (variant 2.1),
- heating highly pressurized water (variant 2.2),
- generation of saturated steam (variant 2.3),
- generation of wet steam, vapor share $x=0.9$ (variant 2.4),
- generation of superheated steam (variant 2.5).

¹ Direct Normal Irradiance

2.1 Water preheating previous to medium pressure feedwater preheater (Heat Exchanger 6)

Unlike customary power plants, the reference plant uses two feed water pumps: The first one to raise the water pressure up to 30 bar, and a second one to rise the pressure up to 210 bar. The heat exchanger 6 (HE6) is in between both pumps.

Process simulations

In this integration concept a heat exchanger (feed-water preheater) is supported by a solar field (SF), which purely heats water without solar steam generation.

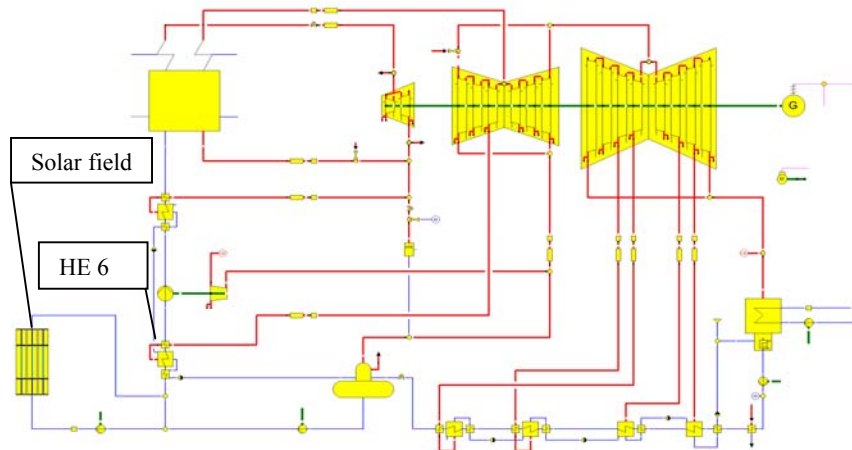


Figure 2: Plant process of the reference plant and feed water preheating with a solar field; solar field heats medium pressurized water (30 bar).

It is the advantage of this “serial” connection (solar field *previous* to HE6) compared to the solar field integration *parallel* to HE6 that the HE6 will automatically provide the amount of heat the solar field is not able to provide. Due to this direct self-control effect, sophisticated multivariable control mechanisms can be avoided. In the simulations, the solar mass flow is adapted in order to keep the solar field outlet temperature constant. In series to the solar field a solar field pump is shown in the block diagram. Depending on the power reserves of the plant’s medium pressure pump, this pump can be omitted. The mass flow through the solar field is controlled by using a bypass in parallel. The mass flow is being entirely led through the bypass (no mass flow through the solar field) when the heat losses in the solar field would exceed the solar heat absorption. The main technical data of the solar field are given in the following table.

Table 1: Solar field parameters

	Parameters
Maximum solar heat input:	30 MW _{th}
Inlet temperature:	172 °C
Outlet temperature:	205 °C
Pressure:	30 bar (pressure before HP-feed-water-pump)
Overall pressure drop:	≈ 4 bar (collector tubes: Ø:15 cm, length: 500 m, up to 742 t/h, tubing to the solar field and back to the power block considered)

The plant is assumed to be operating at full load, whenever solar irradiation is available, besides three weeks of plant revision in January. The live steam parameters, including mass flow, and the intermediate superheating temperature are kept at a constant level, independent of solar energy production. These assumptions lead to supplementary electrical energy and slightly falling gas consumption with increasing solar share (see Figure 3, left diagram).

The resulting efficiency is shown in Figure 3 on the right diagram.

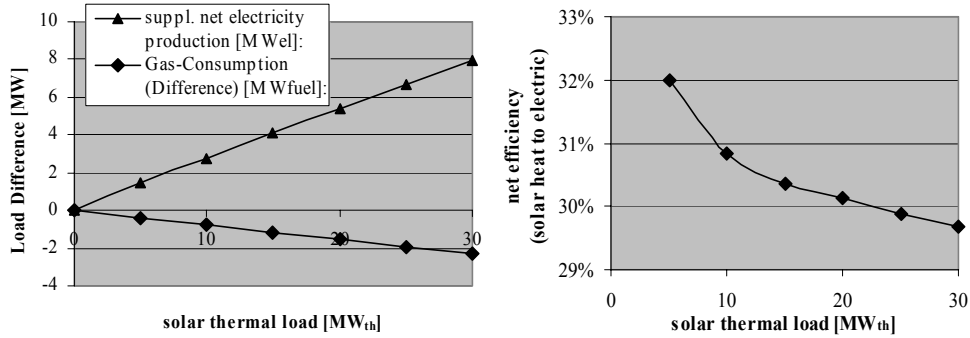


Figure 3: Left diagram: supplementary electricity production (net) and fuel savings, as a function of solar heat production. Right diagram: solar heat efficiency

The solar heat efficiency (Figure 3, right diagram), resulting from the additional electricity production and from the fuel savings, is defined as:

$$\eta_{solar_heat} = \frac{P_{el_net, solar}}{\dot{Q}_{solar}} \quad (1)$$

with the variables:

$$P_{el_net, solar} = P_{el_net} - P_{el_net, ref_plant} + \eta_{net, ref_plant} \cdot (\dot{Q}_{fuel, ref_plant} - \dot{Q}_{fuel}) \quad (2)$$

- \dot{Q}_{solar} : solar heat into the power cycle [MW_{th}]
- $P_{el,net}$: net electric power of the hybrid plant [MW_{el}]
- P_{el_net, ref_plant} : net electric power of the conventional reference plant [MW_{el}]
- η_{net, ref_plant} : efficiency of the conventional reference plant, fuel to net electricity (42.0%)
- $\dot{Q}_{fuel, ref_plant}$: fuel consumption of the conventional reference plant [MW_{fuel}]
- \dot{Q}_{fuel} : fuel consumption of the hybrid plant [MW_{fuel}]

The solar heat efficiency decreases slightly from 32.0% to 29.7% with increasing solar share (see Figure 3). This is due to the fact that the overall plant efficiency decreases with heat input at lower temperatures. The solar field reduces the average heating temperature, since the vessel itself realizes higher temperatures. For this thermodynamic reason the solar energy should preferably be fed into the water-steam-cycle at high temperatures.

Equations 1 and 2 ensure that all energetic effects caused by the solar field are assigned to the solar field. Although the overall efficiency drops slightly through solar hybrid operation, up to additional 8 MW_{el} are provided by the plant because of the solar field.

Electrical yield based on annual irradiation data

Based on the process simulation data and on irradiation data from Meteonorm [3] for the location Kuraymat, Egypt (DNI: 2,306 kWh·m⁻²·a⁻¹), simulations on the annual yield of the hybrid plant were carried out. For this calculation the collector simulation program ColSim [4] was used. This program calculates the thermal and electrical plant yield and is used to optimize the collector design. The optimized Fresnel collector used for these simulations has 48 mirrors, each 50 cm wide, the distance between the mirrors is

constantly 20 cm, the absorber tube has an outer diameter of 150 mm and an absorber height – above the primary mirrors – of 12.3 m.

The annual solar efficiency $\eta_{DNI \rightarrow el, net}$ is defined as:

$$\eta_{DNI \rightarrow el, net} = \frac{E_{el, net, solar}}{A_{mirror} \cdot DNI} \quad (3)$$

with the variables:

$$E_{el, net, solar} = E_{el, net} - E_{el, net, ref_plant} + \eta_{net_ref_plant} \cdot (Q_{fuel, ref_plant} - Q_{fuel}) \quad (4)$$

A_{mirror} : collector surface (resp. cumulated mirror surface of the primary mirrors) [m^2]
 DNI : direct normal irradiance [$kWh \cdot m^{-2} \cdot a^{-1}$]
 $E_{el, net}$: annual net electricity production of the hybrid plant [$MWh_{el} \cdot a^{-1}$]
 E_{el, net, ref_plant} : annual net electricity production of the reference plant [$MWh_{el} \cdot a^{-1}$]
 Q_{fuel, ref_plant} : annual fuel consumption of the reference plant [$MWh_{fuel} \cdot a^{-1}$]
 Q_{fuel} : annual fuel (gas) consumption of the hybrid plant [$MWh_{fuel} \cdot a^{-1}$]

The solar net electricity production as well as the annual solar efficiency (DNI \rightarrow net Electricity) are given in the following two graphs.

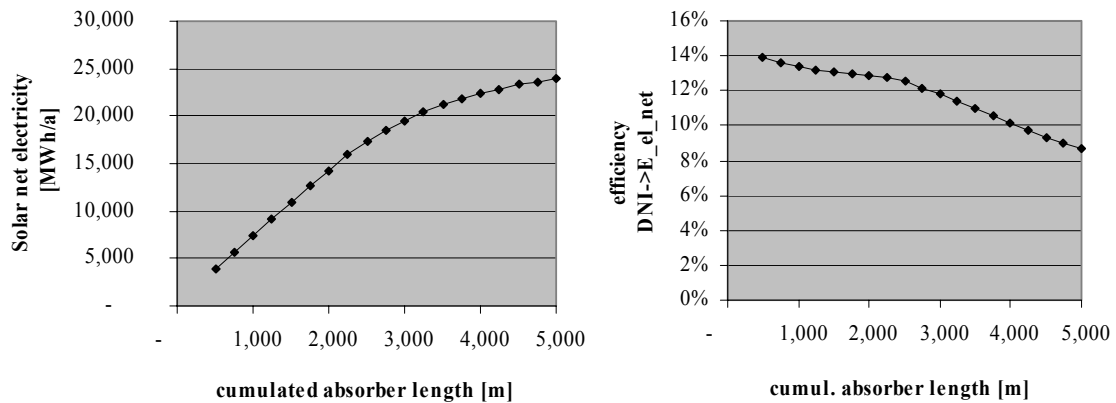


Figure 4: Left diagram: Solar electricity yield depending on cumulated absorber length (several collectors used in parallel), collector width: 24 m of mirrors. Right diagram: Efficiency, fraction of net solar electricity and DNI.

For lower collector lengths, the electricity production is approximately linear to the absorber length (left diagram). The solar heat input was restricted to 30 MW_{th}. Therefore, dumping of solar energy occurs during hours with high solar irradiation for lengths greater than approximately 2,500 m. The annual solar efficiency (DNI \rightarrow net Electricity), Figure 4, right diagram, decreases with increasing solar field sizes. Reasons for that are the decreasing solar heat efficiency (see Figure 3) and, with lengths > 2,500 m, the additional dumping effects.

Economic analysis

The economic assumptions for the following calculations are given in Table 2. Starting point was an assessment of the Solarmundo collector for a developing country (esp. lower wages for construction and operation). In order to assess the technology in a commercial situation, the cost assumptions apply for the second or third collector to be built, having overcome the unexpected difficulties related to new technologies and having gained experience with the administrative and financing processes of solar thermal power plant projects.

Table 2: Economic assumptions for the “third” Fresnel collector field

Investment costs:	
Total Solar field investment ²	Investment = 122 €/m ² x 304,100 m ² x (A / 304,100 m ²) ^{0.93} ⇒ 154 €/m ² (12,000 m ²) down to 129 €/m ² (139,000 m ²)
Annual solar field costs:	
Insurance	1% of solar field investment
Operation and Maintenance:	2% of solar field investment
Natural gas (fuel saving):	1 €/kWh
Financial boundary conditions:	
Interest rate	8%
Lifetime	25 years

For the calculation of the levelized electricity costs the following formula is used:

$$LEC_{solar} = \frac{\text{annuity factor} \times SF \text{ invest} + \text{insurance} + O \& M - \text{fuel savings} - CO_2 \text{ savings} \times \text{allow.price}}{E_{el_net, solar}} \quad (5)$$

The solar LEC in dependence of the solar field size and for different assumptions on CO₂-allowances is given in the following graph.

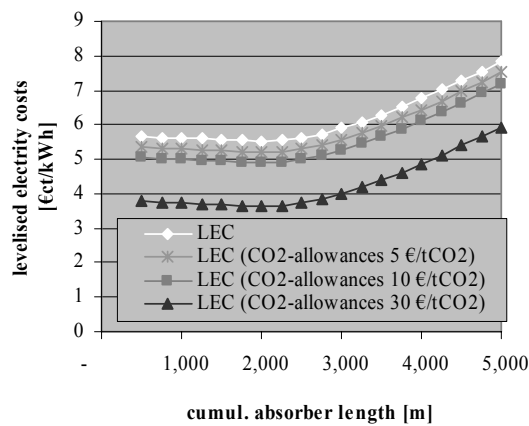


Figure 5: Levelized electricity costs for different assumptions on CO₂-allowances

The cost optimal absorber length is 2,000 m (mirror surface: 48,000 m²). This is the solar field size that realizes the minimal LEC, summarizing two effects that occur with increasing solar field sizes: decreasing efficiency (see Figure 4) and decreasing specific collector costs (see Table 2). The corresponding LEC-optimized collector costs 6.7 million €. The levelized electricity costs of this variant are considerably low: below 6 €/kWh at a site with a DNI of 2,306 kWh·m⁻²·a⁻¹. One reason for such low electricity costs is the

² The formula leads to reduced specific costs for large units.

relatively low investment for the Fresnel collector compared to other solar thermal power technologies. The second reason is that no additional power block investment, related to the solar field, is necessary for the examined variants. This advantage is not technology-specific to the Fresnel-collector but would also apply for the integration of other solar thermal collectors, such as the parabolic trough collector.

CO₂ emissions trading – for instance within the Clean Development Mechanism of the Kyoto Protocol – helps to lower the LEC, as shown for different assumptions on CO₂ allowance prices. But the LEC-reducing effect of CO₂ allowances is not very strong for prices below 10 €/tCO₂, especially since administrative costs – like base-line study, acknowledgement by UNFCCC-committee, etc. – are not taken into consideration in this calculation. Higher certificate prices than 10 €/tCO₂ seem unrealistic from the vantage point of the present.

2.2 Water preheating previous to high pressure preheater (HE 7)

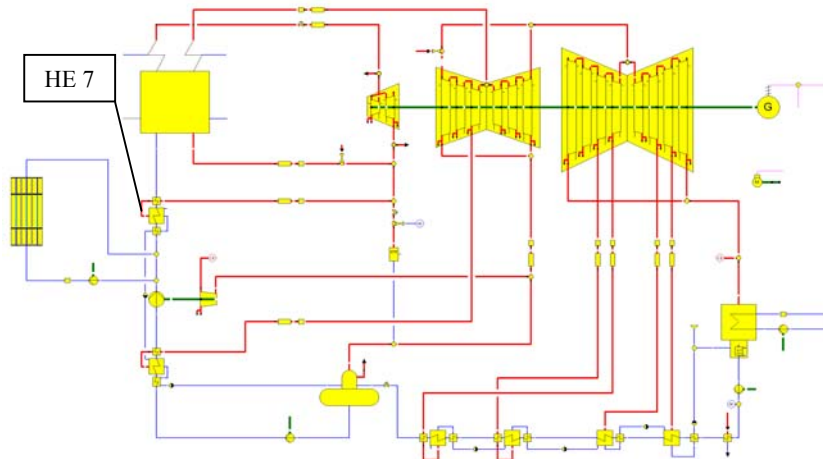


Figure 6: Plant process, solar field heats highly pressurized water (215 bar)

This variant is similar to the previous one, because it also "only" heats water and is connected in series to the preheater with a bypass to control the solar field mass flow. The main differences are the higher solar field parameters (esp. pressure), given in the following table.

Table 3: Solar field parameters

	Parameters
Maximum solar heat input:	30 MW _{th}
Inlet temperature:	207 °C
Outlet temperature:	270 °C
Pressure:	215 bar (pressure after HP-feed-water-pump)
Nominal mass flow:	371 t/h

In order to handle the high pressure in the solar field, thicker tubes are necessary than for the medium pressure water heating variant. According to a first assessment the thickness of the tube would be 9 mm (diameter: 150 mm, steel: 13CrMo44).

The resulting solar heat efficiency (water-steam-cycle simulations) and the solar LEC³ (depending on the solar field size) are given in the next two diagrams. Due to the higher efficiency, the LEC is 1 €/ct/kWh_{el} below the variant 2.1.

³ For all examined variants, the same specific collector costs (€/m²) were assumed. For this high-pressure-variant higher costs for the pipes and the SF pump are expected than for the previously described concept. The used cost-model includes collector tubes (resp. tube costs in €/m) with an outer diameter of 220 mm and a tube thickness of 13 mm, the assumed steel is 13CrMo44.

The solar heat efficiency and the resulting solar LEC of the high pressure solar water heating concept are given in the next two graphs.

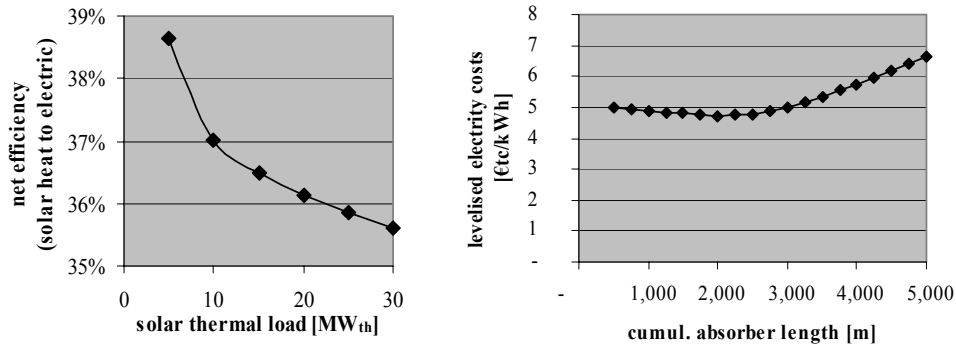


Figure 7: Solar heat efficiency (left diagram) and solar LEC without CO₂-allowances taken into account (right diagram)

2.3 Saturated solar steam generation fed into HE 7

In this variant the solar heat is led into the preheater as saturated steam, instead of introducing the heat on the water side of the preheater.

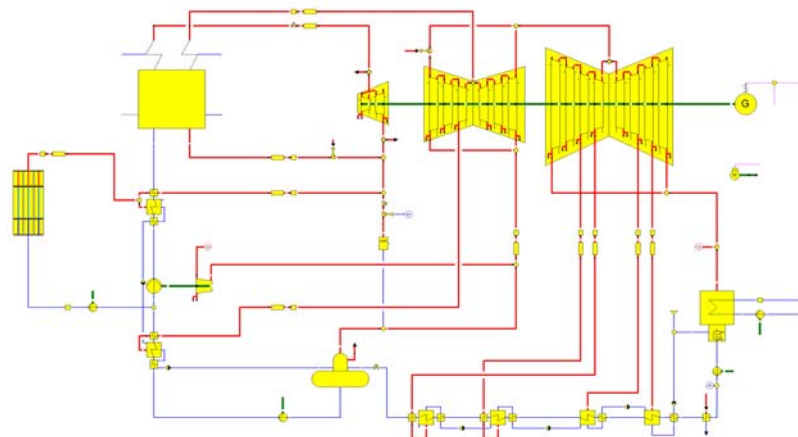


Figure 8: Plant process, solar field provides saturated steam for HE7

Table 4: Solar field parameters

	Parameters
Maximum solar heat input:	30 MW _{th}
Inlet temperature:	202 °C
Outlet temperature:	254 °C (saturated steam)
Pressure:	42 bar (pressure before reheating section)
Nominal mass flow:	65 t/h

The solar heat efficiency depending on solar heat production of the variants 2.2-2.5 are almost the same, because in all variants the solar field is used in order to substitute extraction steam from the high pressure turbine. Therefore the corresponding graphs are not shown again. In a comparative assessment of the technologies the levelised electricity costs of all variants as well as relevant technical aspects will be discussed (see chapter 3).

2.4 Wet steam (vapor share $x=0.9$) fed into HE7

The plant process of solar wet steam variant is like in variant 2.3. Here the water in the solar field is not entirely vaporized at the outlet of the solar field. This allows avoiding a recirculation pump, which is necessary for the distinct division of the collector into a vaporizing section and a superheating section. This collector division is pursued to reduce material stress in the collector tubes.

Table 5: Solar field parameters

	Parameters
Maximum solar heat input:	30 MW _{th}
Inlet temperature:	202 °C
Outlet temperature:	255 °C (wet steam, $x=0.9$)
Pressure:	43 bar
Nominal mass flow:	61 t/h

2.5 Superheated solar steam fed into cold intermediate superheating section

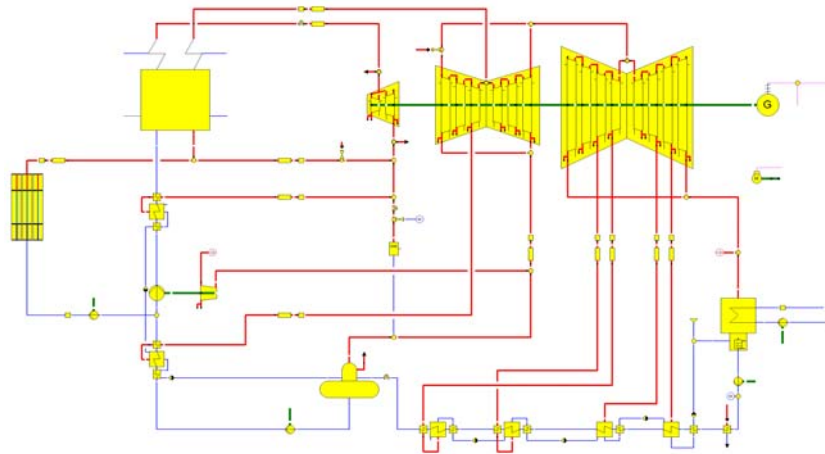


Figure 9: Plant process, solar field provides steam for the cold reheating section

This is the only analyzed concept where the solar field is used with its three sections for preheating, vaporizing and superheating of steam. The solar steam is then fed into the cold reheating section.

Table 6: Solar field parameters

	Parameters
Maximum solar heat input::	30 MW _{th}
Inlet temperature:	202 °C
Outlet temperature:	339 °C (superheated steam)
Pressure:	42 bar
Nominal mass flow:	49 t/h

3. Discussion

Five variants of integrating 30 MW_{th} of solar heat, provided by a Fresnel collector, into a 630 MW_{el} gas power plant were investigated – two for water heating and three for steam generation. Efficiencies and additional electricity production costs of the solar part were calculated. The main results of the simulations are shown in the table below.

Table 7: Simulation results

variant	levelized electricity costs ⁴	cost optimal solar field size (tube length / mirror surface)	investment	annual Efficiency (E _{el,net} / DNI)	annual heat eff. (E _{el,net} / Q _{solar})	solar share (E _{el,solar} / E _{el,total})
Med. pressurized water heating (2.1)	5.5 €/ct/kWh	2,000 m / 48,000 m ²	6.7 million €	12.9%	30.6%	0.3%
High pressure water heating (2.2)	4.7 €/ct/kWh	2,000 m / 48,000 m ²	6.7 million €	15.0%	36.4%	0.3%
Saturated steam generation (2.3)	4.9 €/ct/kWh	2,000 m / 48,000 m ²	6.7 million €	14.8%	35.9%	0.3%
wet steam generation (2.4)	5.0 €/ct/kWh	2,000 m / 48,000 m ²	6.7 million €	14.7%	35.8%	0.3%
superheated steam generation (2.5)	5.2 €/ct/kWh	2,079 m / 49,896 m ²	6.9 million €	14.3%	36.0%	0.3%

Beyond the results given in Table 7, technical risk aspects play an important role for the comparison the variants.

Solar production of superheated steam (Variant 2.5) may be of interest in order to prove the direct steam generation (DSG) in horizontal Fresnel collector tubes. However, from an energetic and economic point of view, the DSG variant is slightly worse than the other integration variants, substituting extraction steam from the high pressure turbine by solar heat (variants 2.2 - 2.4). This concept has higher operational risks because of DSG and superheated steam sections. Therefore this variant bears no advantages compared to other systems and should not be pursued, except for research on direct steam generation.

Solar production of wet steam (Variant 2.4) has a strong advantage compared to solar production of saturated steam (variant 2.3), because it does not need a recirculation pump for the solar field. On the other hand, extra costs may arise because of special tubing needed to lead the two-phase flow from the solar field back to the plant process. The saturated solar steam concept (variant 2.3) also has problems with condensing water in the tubing between the solar field and power plant, however to a lower extent. An advantage of solar wet steam production (variant 2.4) over high pressure solar water heating (variant 2.2) is the lower pressure level in the solar field (42 bar versus 215 bar).

Besides the high pressure in the tubing – which could be handled with thicker tubes – variant 2.2 (HP water heating) is an interesting variant because it has a simple design (no steam generation, simple control mechanisms) and is energetically the best integration concept. On the other hand, it bears high risks due the high pressure level (215 bar). Investment costs will rise (not considered in these calculations) due to thicker tubing and a more stable construction to sustain the 2-3 times heavier tube.

For a first plant concept the medium pressure variant (2.1) is the most favorable one. It profits from the same technical advantages as variant 2.2 (no DSG, simple control mechanisms) and, bears the lowest technical risk. It consists of simple water heating at a moderate pressure level (30 bar). Although it is the variant realizing the highest LEC among the examined concepts, it still reaches a level below 6 €/ct/kWh. (DNI: 2306 kWh·m⁻²·a⁻¹).

⁴ Same specific costs for the solar field assumed, regardless of differences concerning tube properties, control aspects, pumps and other differing necessities. The assumed solar field costs include the feed water pump and a recirculation pump.

4. Summary and Conclusions

It has been shown that it is energetically more advantageous to heat water than to produce steam in the solar collector. Furthermore, for successful market introduction, it is important to offer a reliable system. Therefore, for the first introduction, the medium pressure water preheating variant (variant 1) is the most favorable variant among the five suggested plant concepts. It does generate slightly higher leveled electricity costs, but from the vantage point of the present, it bears almost no technical risks.

In a second step, either the high pressure water heating variant or the wet steam generating collector, depending on the results of a more detailed analysis, will be more economical and thus more attractive.

However, only limited amounts of solar energy can be fed into an existing power plant without extra power cycle investment. This significantly limits the solar share. Therefore the long term strategy should aim at producing live steam with the solar field (temperatures $> 500^{\circ}\text{C}$). Then a conventional boiler and the solar field can be used in parallel and the boiler will supply the thermal energy, the solar field cannot provide.

5. References

- [1] Lerchenmüller, Mertins, Morin, Häberle, Zahler, Ewert, Fruth, Griestop, Bockamp, Dersch, Eck (2004): final project report, funded by the German Federal Ministry for the Environment (ZIP program): “Technische und wirtschaftliche Machbarkeits-Studie zu horizontalen Fresnel-Kollektoren”
- [2] Ebsilon, Process simulation tool developed by Sofbid, <http://www.sofbid.com>
- [3] Meteonorm, meteorological database developed by Meteotest, <http://www.meteotest.ch>
- [4] Mertins, Lerchenmüller, Häberle (2004): “Geometry Optimization of Fresnel-Collectors with economic assessment”, 5th ISES Europe Solar Conference, EuroSun2004